Applied Physics Research; Vol. 10, No. 6; 2018
ISSN 1916-9639 E-ISSN 1916-9647
Published by Canadian Center of Science and Education

Vector Analysis and Optimal Control for the Voltage Regulation of a Weak Power System with Wind Energy and Power Electronics

Nick Schinas[1]

[1] Technological Educational Institute of Western Greece, Patras, Greece

Correspondence: Nick Schinas, Technological Educational Institute of Western Greece, Patras, Greece. E-mail: nickschinas@gmail.com, nschinas@teiwest.gr

Received: September 14, 2018 Accepted: October 1, 2018 Online Published: November 30, 2018

doi:10.5539/apr.v10n6p1 URL: https://doi.org/10.5539/apr.v10n6p1

Abstract

This paper deals with the voltage regulation in a weak system which contains large inductive loads and wind turbines using Doubly Fed Induction Generators (FDIGs). The DFIGs demand large amounts of reactive power from the grid and as a result, there is a voltage drop in the system which may be extra deteriorated if large inductive loads and motors are also present in the same line. The problem of the voltage regulation in these cases is treated with the installation of a Static Var Compensator (SVC) besides the capability of the DFIGs to partially regulate the voltage themselves. In this paper, new modeling procedures based on optimal control are developed for the design of the SVC controller and a novel strategy for the grid side converter of the DFIG is presented. The nonlinear system is simulated in the SIMULINK software so that the performance of the new controllers is validated.

Keywords: wind turbine, voltage regulation, doubly fed induction generator, optimal control.

1. Introduction

The increased need for wind energy development makes the installation of wind turbines in 'weak' ac grids necessary. On the other hand, many voltage instability incidents have taken place around the world the last years (Custem & Vournas, 1998; Berizzi, 2004). The distributed generation with wind power stations installed in weak distribution systems may enlarge this problem especially when large inductive loads are connected to the same line. So, voltage regulation has become a major research area in the field of power systems (Chondrogiannis, 2007; Ledesma, 2002; Kesraoui, 2016).

This paper deals with the design of the necessary control loops so that good performance of the grid voltage can be attained in a very weak system which contains a wind park (WP) and large inductive loads. The WP consist of wind turbines with Doubly Fed Induction Generators (DFIGs). The DFIGs demand reactive power from the grid. These amounts of reactive power make the grid voltage very sensitive to load variations. The voltage performance can be improved by means of FACTS devices and better voltage controllers inside the DFIG.

The system under study is shown in Figure 1. A medium voltage line is connected to the main grid at bus 1 with short circuit capability of 150 MVA. There is a steam power generation system (SPGS) at bus 2 with rated power of 50 MVA and a wind park at bus 3 connected to this line. This system can be a part of a local grid in an island to which wind parks are to be installed.

The WP includes 11 wind turbines each with rated real power of 1.5 MW. At bus 4 there are inductive loads with rated power of 2 MVA and power factor 0.9 lagging. These loads also include three asynchronous motors each rated 300 kW. The nominal line voltage of the system is 25 kV. The variation of the reactive power demanded from the WP causes the load voltage at all buses to deviate from the rated values despite the presence of the SPGS in the system. At t = 50 sec there is an increase in the wind speed from 8 m/s to 14 m/s and at t = 75 sec the large induction motors start to operate. Figure 2 shows the rms value of the load voltage at bus 4. The real power produced from the WP is shown in Figure 3 and the reactive power from the WP is shown in Figure 4. The real power production of the SPGS is kept constant at 15 MW.

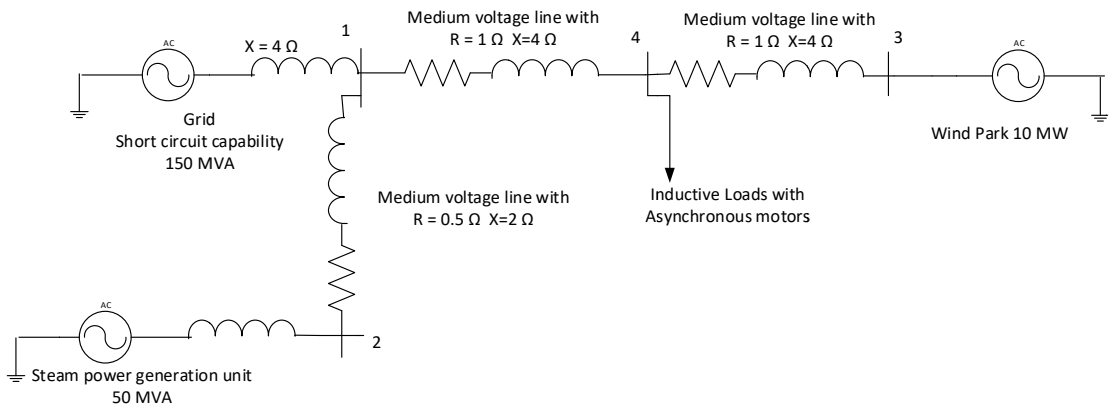

Figure 1. System under study

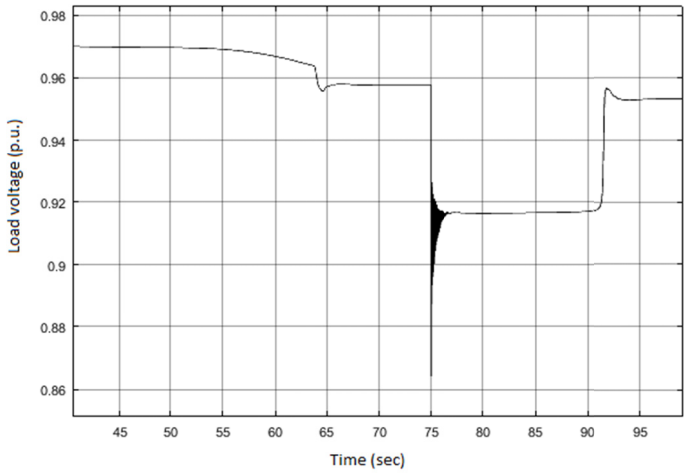

Figure 2. RMS load voltage in p.u.

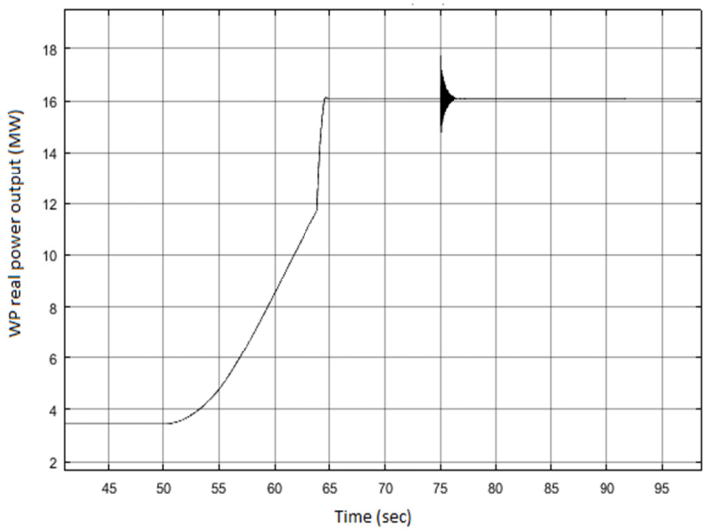

Figure 3. Real power from the WP (MW)

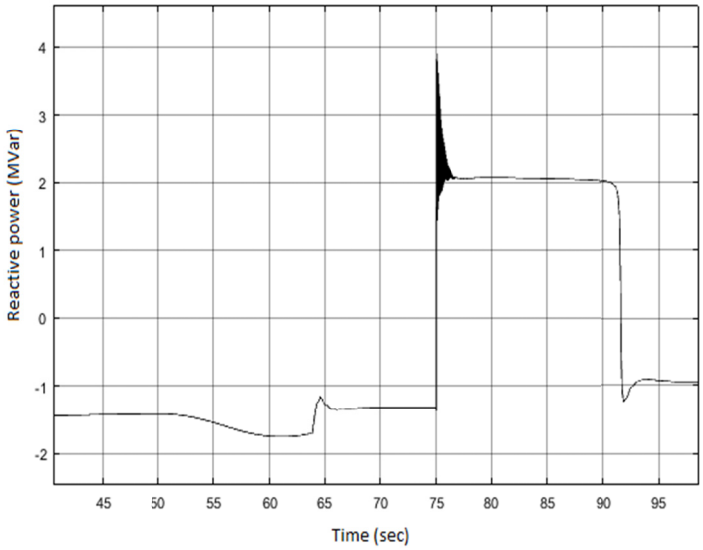

Figure 4. Reactive power from the WP in MVars

As we can see, the grid voltage starts to decrease from the rated value when the wind speed increases due to the fact that the reactive power from the grid towards the WP increases. From t = 50 sec up to t = 70 sec the WP causes a voltage drop of about 2 % to the system. The grid voltage decreases significantly during the start of the asynchronous motors in which the reactive power exchange between the grid and the WP changes direction. This change in the direction of the reactive power stresses the various electronic components of the system especially those of the wind turbines. Finally, the steady state voltage drop to the load bus after the insertion of the motors is about 5% while without the presence of the WP the steady state voltage drop would be 3%.

What happens if we try to add one more wind turbine into the system? Figure 5 shows the rms load voltage after the insertion of the motors and Figure 6 shows the real power coming from the WP. We can see that the load voltage takes very low values now and there is a serious oscillation after the start of the motors. The real power from the WP also oscillates and does not increase. This actually means that this wind turbine cannot be connected to the line.

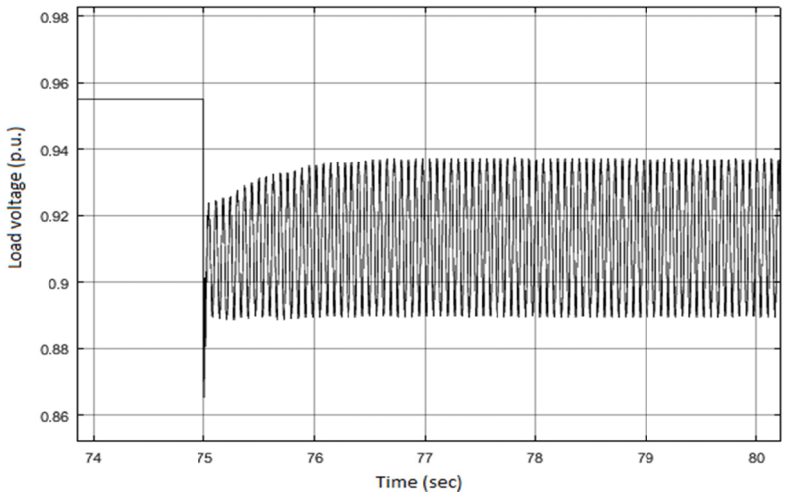

Figure 5. Load voltage with 12 wind turbines

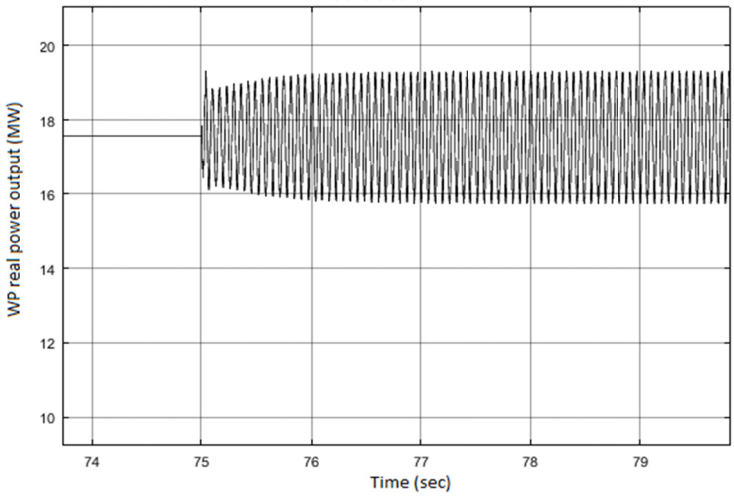

Figure 6. Real power from the WP with 12 wind turbines

The improvement of the grid voltage performance can be achieved by means of the installation of a Static Var Compensator (SVC) at the bus 1 and the proper design of the current regulator of the grid-side controller of the WT. The purpose of this paper is the presentation of new methods based on optimal control theory for the design of the SVC controller and the grid-side controller of the WT so that the right amounts of reactive power are injected into the system to stabilize the voltage. As we shall see, the improved performance of the voltage permits two more wind turbines to be connected to the line which means that higher penetration of wind energy can be accomplished in weak systems if good voltage regulation is achieved.

2. Description and modeling of the system

2.1 Mathematical model of the generator and the power line between the buses 1-2

The mathematical model in p.u. of the synchronous generator (SG) of the SPGS is (Padiyar, 2014):

$$\frac{1}{\omega_s}\frac{d\psi_d}{dt} = R_s i_d + \frac{\omega}{\omega_s}\psi_q + v_d \quad \text{(a)}$$

$$\frac{1}{\omega_s}\frac{d\psi_q}{dt} = R_s i_q - \frac{\omega}{\omega_s}\psi_d + v_q \quad \text{(b)}$$

$$T'_{do}\frac{dE'_q}{dt} = -E'_q - (X_d - X'_d)i_d + E_{fd} \quad \text{(1a)}$$

$$T'_{qo}\frac{dE'_d}{dt} = -E'_d + (X_q - X'_q)i_q \quad \text{(2a)}$$

$$\frac{d\delta}{dt} = \omega - \omega_s \quad \text{(3a)}$$

$$\frac{2H}{\omega_s}\frac{d\omega}{dt} = T_m - (\psi_d i_q - \psi_q i_d) - T_D \quad \text{(4a)}$$

where:

ψ_d, ψ_q are the d,q components of the stator magnetic flux respectively,

i_d, i_q are the d,q components of the stator current respectively,

v_d,v_q are the d,q components of the stator voltage respectively,

E'_q, E'_d are the d,q components of the stator internal transient voltage respectively,

X_d ($=X_{ls}+X_{md}$) is the d axis reactance, X_q ($=X_{ls}+X_{mq}$) is the q axis reactance,

X'_d ($= X_d - X^2_{md}/X_{fd}$) is the d axis transient reactance,

X'_q (= X_q - X^2_{mq}/X_{1q}) is the q axis transient reactance,

ω is the rotor electrical angular speed, ω_s is the electrical speed of the magnetic flux,

δ is the power angle, H is the inertia constant,

T_m is the mechanical torque, T_D is the damping torque (being neglected from now on).

Finally, T'_{do}, T'_{qo} are time constants on field and damper winding respectively (we consider the machine to have one damping winding on q axis) and R_s is the stator resistance.

By neglecting the equations regarding the stator magnetic fluxes (equations (a) and (b) above) and replacing the relevant values from the Appendix we have:

$$\frac{dE'_q}{dt} = -0.22\ E'_q - 0.31 i_d + 0.22 E_{fd} \quad (1b)$$

$$\frac{dE'_d}{dt} = -1.5\ E'_d + 1.7\ i_q \quad (2b)$$

$$\frac{d\delta}{dt} = \omega - 314 \quad (3b)$$

It also is:

$$\psi_d = -x'_d i_d + E'_q, \quad \psi_q = -x'_q i_q - E'_d$$

By replacing to (4a) we finally reach in:

$$\frac{d\omega}{dt} = 180.46\ T_m - 180.46\ E'_q i_q - 180.46\ E'_d i_d + 37.89 i_d i_q \quad (4b)$$

As we have already seen, the SPGS is connected to the bus 2 and there is a small line up to the main bus 1. The Figure 7 depicts the vectors of the voltages at the buses. The voltage v_2 at the bus 2 will be a little ahead of the voltage v_1 at the bus 1 (approximately 3 degrees). We consider the main axes D, Q and the axes d, q internally in the synchronous generator to which the various quantities of the SG have been analyzed in the equations (1b)-(4b). We arbitrarily consider that the voltage v_2 is lying on the D axis.

The stator current i of the SG with its components i_d, i_q onto the axes d, q is also the current I of the line between the buses 2 and 1 with the components I_D, I_Q onto the axes D, Q respectively. It is (Pai et al., 2014):

$$i_d = I_D sin\delta - I_Q cos\delta, i_q = I_D cos\delta + I_Q sin\delta \quad (5a)$$

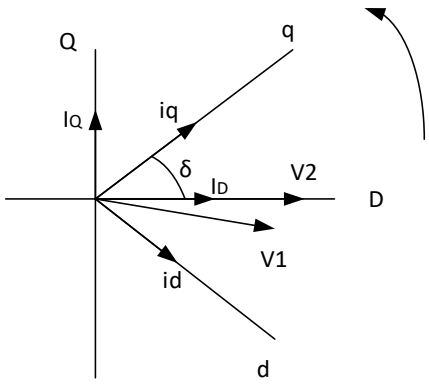

Figure 7. Vector analysis of the system

Applying the D-Q analysis on the line between the buses 2 and 1 we have firstly on the D axis:

$$V_{2D} = V_{1D} + R_{2-1} I_D + L_{2-1} \frac{dI_D}{dt} + X_{2-1} I_Q \Rightarrow V_{2D} - V_{1D} = R_{2-1} I_D + L_{2-1} \frac{dI_D}{dt} + X_{2-1} I_Q$$

Due to the small value of the angle between v_1 and v_2 it is approximately: $V_{2D} - V_{1D} \approx 0$. So from the previous equation we conclude to:

$$L_{2-1}\frac{dI_D}{dt} = -R_{2-1}I_D - X_{2-1}I_Q$$

and by replacing the values from the Appendix we have:

$$\frac{dI_D}{dt} = -0.35I_D - I_Q \quad (5)$$

From the line analysis on the axis Q we have:

$$V_{2Q} = V_{1Q} + R_{2-1}I_Q + L_{2-1}\frac{dI_Q}{dt} - X_{2-1}I_D \Rightarrow V_{2Q} - V_{1Q} = R_{2-1}I_Q + L_{2-1}\frac{dI_Q}{dt} - X_{2-1}I_D$$

By taking into account that $v_{2Q} = 0$ and by replacing the values we have:

$$\frac{dI_Q}{dt} = -0.35I_Q + I_D - 3.8V_{1Q} \quad (6)$$

The equations (1b)-(4b) can be rewritten if we replace the quantities i_d, i_q by I_D, I_Q using the equation (5a). Then we can reach in:

$$\frac{dE'_q}{dt} = -0.22E'_q - 0.31I_D sin\delta + 0.31I_Q cos\delta + 0.22E_{fd} \quad (1)$$

$$\frac{dE'_d}{dt} = -1.5E'_d + 1.7I_D cos\delta + 1.7I_Q sin\delta \quad (2)$$

$$\frac{d\delta}{dt} = \omega - 314 \quad (3)$$

$$\frac{d\omega}{dt} = 180.46T_m - 180.46E'_q I_D cos\delta - 180.46E'_q I_Q sin\delta - 180.46E'_d I_D sin\delta + 180.46E'_d I_Q cos\delta -$$
$$-18.95I_D^2 sin2\delta + 18.95I_Q^2 sin2\delta - 37.89I_D I_Q sin^2\delta + 37.89I_D I_Q cos^2\delta \quad (4)$$

The nonlinear system that consists of the voltage v_1 at the bus 1 and the internal quantities of the SG is actually described by the equations (1)-(6). By linearizing the above equations around the operating point given at the Appendix we finally conclude to the linear system given by the following equations:

$$\frac{d\Delta E'_q}{dt} = -0.22\Delta E'_q - 0.06\Delta\delta - 0.155\Delta I_D + 0.27\Delta I_Q + 0.22\Delta E_{fd} \quad (7)$$

$$\frac{d\Delta E'_d}{dt} = -1.5\Delta E'_d - 0.385\Delta\delta + 1.47\Delta I_D + 0.85\Delta I_Q \quad (8)$$

$$\frac{d\Delta\delta}{dt} = \Delta\omega - 314 \quad (9)$$

$$\frac{d\Delta\omega}{dt} = -37.45\Delta E'_q - 40.89\Delta E'_d + 20.7\Delta\delta + 137.2\Delta I_D - 25\Delta I_Q + 180.46\Delta T_m \quad (10)$$

$$\frac{d\Delta I_D}{dt} = -0.35\Delta I_D - \Delta I_Q \quad (11)$$

$$\frac{d\Delta I_Q}{dt} = -0.35\Delta I_Q + \Delta I_D - 3.8\Delta V_{1Q} \quad (12)$$

The equations (7)-(12) form the linearized model of the SG and the line between the buses 1 and 2.

2.2 Model of the grid – side converter of the WT

A schematic configuration of the grid side converter, is shown in Figure 8 in which the grid phase voltages are denoted as e_a, e_b, e_c and the converter phase voltages as v_a, v_b, v_c are respectively. The d,q components (i_d, i_q) of the line currents i_a, i_b,i_c concerning the d,q components (v_d, v_q) of the converter voltages v_a, v_b, v_c can be given by the following equations (Vittal & Ayyanar, 2013):

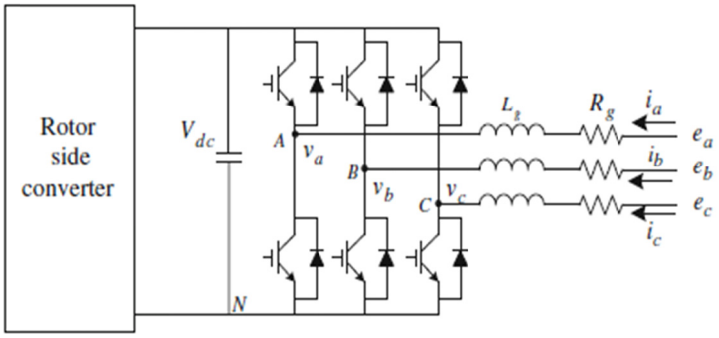

Figure 8. Grid side converter configuration (Vittal & Ayyanar, 2013)

$$L_g \frac{di_d}{dt} = -R_g i_d + \omega_s L_g i_q + e_d - v_d, \quad L_g \frac{di_q}{dt} = -R_g i_q - \omega_s L_g i_d - v_q$$

The modeling of the converter of the WT and its control design has nothing to do with the rest of the system, so the choice of the WT d,q, axes is arbitrary. The grid voltage e has been chosen to lie on the d axis and so $e_q = 0$. By replacing the p.u. values from the Appendix we reach in the following equations:

$$\frac{di_d}{dt} = -0.01 i_d + i_q + 6.67 e_d - 6.67 v_d, \quad \frac{di_q}{dt} = -0.01 i_q - i_d - 6.67 v_q$$

As there is the SPGS in our system with installed capacity much larger that the rated output of the WP, the frequency is assumed to be constant and that it does not depend on the real power coming from the WP. As a result, the parameter ω_s has been set equal to 1. Besides, the parameter e_d is considered to be a disturbance for the control system and not an input and so the linearized model for the control design of the grid side converter is given by:

$$\frac{d\Delta i_d}{dt} = -0.01 \Delta i_d + \Delta i_q - 6.67 \Delta v_d, \quad \frac{d\Delta i_q}{dt} = -0.01 \Delta i_q - \Delta i_d - 6.67 \Delta v_q \tag{13}$$

3. Control SYSTEM DESIGN

3.1 SVC Controller Design

In order for the load voltage to be kept constant under reactive power from the WP and the load variations, an SVC installation is proposed at the bus 1 of the system. The SVC is actually a device with variable susceptance through which fast power factor improvement can be achieved. Figure 9 shows a typical SVC (TSC-TCR) configuration. There is a main voltage controller which according to the deviation of the bus voltage from the rated value regulates the right susceptance being connected to the bus and so the right amount of reactive power being inserted into the system. A block diagram of SVC voltage control is depicted in Figure 10. There can be more auxiliary signals in the decision of the right susceptance (B) of the SVC control, like the signals V_s shown in Figure 10. There are no such signals in our study. The connected susceptance at the bus 1 will force the magnitude of the voltage at the bus 1 to change. If only the fundamental component of Vsvc is considered, we can assume that:

$$\Delta V_{svc} \cong X \Delta B_{svc},$$

that is, the variation of the magnitude of the voltage at the bus where the SVC is installed (i.e. bus 1) depends on the variation of the susceptance of the SVC (ΔBsvc). X is the equivalent Thevenin resistance of the grid as seen from the bus 1.

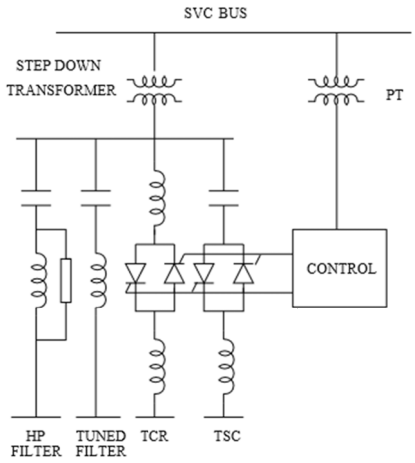

Figure 9. Typical configuration of SVC (TSC-TCR) configuration (Padiyar, 2014)

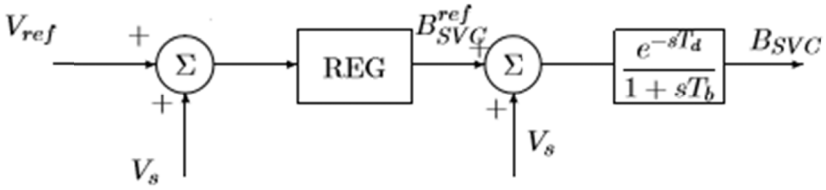

Figure 10. SVC voltage control with series regulator (Padiyar, 2014)

The equations (7)-(12) form the linearized model concerning the SPGS and the line between the buses 1 and 2. The SPGS is considered to produce steady real power into the system and so the angle δ_1 is almost constant, that is:

$$V_{1Q} = |V_1| sin\delta_1 \Rightarrow \Delta V_{1Q} = sin\delta_{1o} |\Delta V_1| \Rightarrow \Delta V_{1Q} = sin\delta_{1o} V_{1o}\, X\, \Delta B_{svc} \Rightarrow \Delta V_{1Q} = 0.035 \Delta B_{svc} p.u.$$

In the model given by (7)-(12) the input to the system will actually be the change in the susceptance ΔB_{svc} but we set for now as input the variation of the voltage ΔV_{1Q} and the calculated input will be transformed into the equivalent susceptance value in the end.

For the output to be selected, we need a signal that will follow the voltage variation. As we can see from Figure 11, the q-axis component of the stator current i_q of the synchronous generator has the same performance as the load voltage. From the equation (5a) it is:

$$i_q = I_D cos\delta + I_Q sin\delta.$$

By linearizing we get:

$$\Delta i_q = 0.866 \Delta I_D + 0.5 \Delta I_Q - 0.21 \Delta\delta \quad (14)$$

So, in the linearized model of the equations (7)-(12) the equation (14) regarding the output of the system must be added. The equations (7)-(12) and the equation (14) form a system of 6th order. By means of MATLAB software, we can reach in a new 2nd order system which is equivalent to the previous one. The new system is given in state – space form $\dot{x} = Ax + Bu, y = Cx + Du$:

$$A = \begin{bmatrix} -0.5246 & 0 \\ 0 & 4.857 \end{bmatrix}, B = \begin{bmatrix} 1.219 \\ -0.0225 \end{bmatrix}, C = [-1.219\ 3.025], D = 0,\ x = \begin{bmatrix} x_1 \\ x_2 \end{bmatrix} \quad (15)$$

The design of the SVC controller is based on the optimal control theory. We want the variations of the state variables and the output to be minimized within a specific smalltime period (t_f). So, the following performance index has been set:

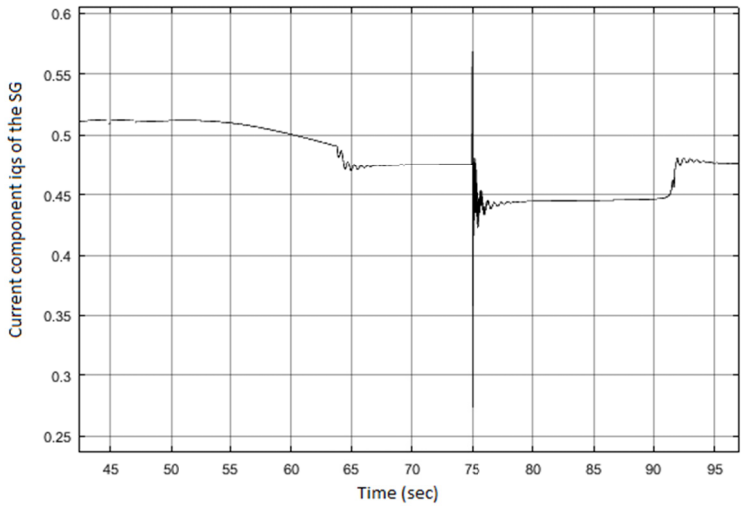

Figure 11. Q-axis component of the current from the SG (p.u.)

$$J = \frac{1}{2}\int_0^{t_f} (x_1^2(t) + x_2^2(t) + u^2(t))dt$$

which is of the form:

$$J = \frac{1}{2}x^T(t_f)F(t_f)x(t_f) + \frac{1}{2}\int_0^{t_f} [x^T(t)Q(t)x(t) + u^T(t)R(t)u(t)]dt$$

with F = 0, R = 1 and $Q = \begin{bmatrix} 1 & 0 \\ 0 & 1 \end{bmatrix}$. According to the optimal control theory, the following matrix differential Riccati equation needs to be solved:

$$\dot{P} = -P(t)A(t) - A(t)^T P(t) + P(t)B(t)R^{-1}B(t)^T P(t) - Q(t)$$

where:

$P = \begin{bmatrix} p_{11} & p_{12} \\ p_{12} & p_{22} \end{bmatrix}$, with final condition P ($t = t_f$) = F = 0.

The optimal input u is then:

$$u(t) = -Kx(t), \text{ with } K=R^{-1}B(t)^T P(t). \quad (16)$$

From the previous definitions and the matrices A, B, C, D given in equation (15), we finally have the following differential equations for the various elements of the matrix P:

$$\dot{p_{11}} = 1.049p_{11} + 1.486p_{11}^2 - 0.0548p_{11}p_{12} + 0.0005p_{12}^2 - 1,$$
$$\dot{p_{12}} = -4.3324p_{12} + 1.4586p_{11}p_{12} - 0.0274p_{12}^2 + 0.0005p_{12}p_{22}$$
$$\dot{p_{22}} = -9.714p_{22} + 1.486p_{12}^2 - 0.0548p_{12}p_{22} + 0.0005p_{22}^2 - 1$$

We set the time interval t_f equal to 1 sec. Solving the previous set of equations for time interval longer than 1 sec (such as 4 sec) we can see that the parameters p_{11}, p_{12}, p_{13} are: $p_{11} = 0.55$, $p_{12} = 0$, $p_{22} = 190000$. So, the state feedback array K is equal to: K = [0.67 -4275]. According to the equation (16) the optimal control input for the SVC controller should be:

$$u = -0.67x_1 + 42752x_2$$

By transforming this input to the real input ΔB_{SVC} and by means of MATLAB software, the equivalent series controller (as it is shown in Figure 10) is:

$$G_c(s) = \frac{-62.52s^2 + 273.8s + 145.2}{s^2 - 9.478s + 22.44} \quad (17)$$

We can see the step response of the linearized model with the optimal control input given by the equation (17) in Figure 12.

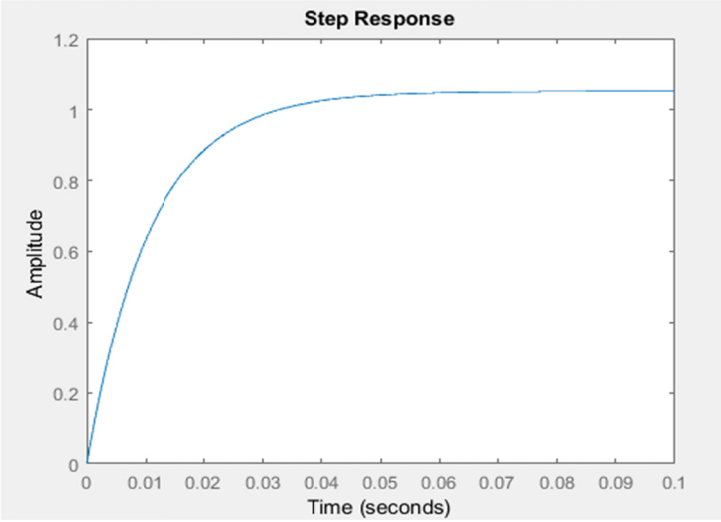

Figure 12. Step response of the linearized model under optimal control.

We can see that the system output gets the desired value in 0.1 sec.

3.2 Grid side converter control design

The linearized model is given by the equations (13). In state space form if we set

$$x = \begin{bmatrix} x_1 \\ x_2 \end{bmatrix} = \begin{bmatrix} \Delta i_d \\ \Delta_{i_q} \end{bmatrix}, u = \begin{bmatrix} u_1 \\ u_2 \end{bmatrix} = \begin{bmatrix} \Delta v_d \\ \Delta v_q \end{bmatrix}, \text{ then we can write:}$$

$$\dot{x_1} = -0.01x_1 + x_2 - 6.67u_1 = f_1, \qquad \dot{x_2} = -0.01x_2 - x_1 - 6.67u_2 = f_2$$

Due to the nature of the above equations we can work with the Hamilton - Jacobi – Bellman (HJB) equation and conclude to a controller very easily. We set the performance index as:

$$J = \int V\big(x(t), u(t)\big)dt = \int (x_1^2 + x_2^2 + u_1^2 + u_2^2)dt$$

and we consider the optimal performance index to

be equal to: $J^* = \frac{1}{2}kx_1^2 + \frac{1}{2}kx_2^2$, then it is: $J_x^* = \begin{bmatrix} \frac{\partial J^*}{x_1} \\ \frac{\partial J^*}{x_2} \end{bmatrix} = \begin{bmatrix} kx_1 \\ kx_2 \end{bmatrix}$, $J_t^* = \frac{\partial J^*}{\partial t} = 0$.

We set the Hamiltonian equation as:

$$H(x(t), u(t), J_x^*) = V\big(x(t), u(t)\big) + J_x^{*T}\begin{bmatrix} f_1 \\ f_2 \end{bmatrix} = x_1^2 + x_2^2 + u_1^2 + u_2^2 + [kx_1\ kx_2]\begin{bmatrix} -0.01x_1 + x_2 - 6.67u_1 \\ -x_1 - 0.01x_2 - 6.67u_2 \end{bmatrix}$$

$$H(x(t), u(t), J_x^*) = x_1^2 + x_2^2 + u_1^2 + u_2^2 - 0.01kx_1^2 - 6.67kx_1u_1 - 0.001kx_2^2 - 6.67kx_2u_2$$

In order to have optimization there must be:

$$\frac{\partial H}{\partial u_1} = 0 \Rightarrow u_1^* = 3.335kx_1, \frac{\partial H}{\partial u_2} = 0 \Rightarrow u_2^* = 3.335kx_2\ .$$

By substitution to the previous we have:

$$H(x(t), u(t), J_x^*) = x_1^2 + x_2^2 + 11.12k^2x_1^2 + 11.12k^2x_2^2 - 0.01kx_1^2 - 0.01kx_2^2 - 22.24k^2x_1^2 - 22.24k^2x_2^2 \Rightarrow$$

$$H(x(t), u(t), J_x^*) = (1 - 11.12k^2 - 0.01k)x_1^2 + (1 - 11.12k^2 - 0.01k)x_2^2$$

We solve the HJB equation:

$$H\big(x(t), u(t), J_x^*\big) + J_t^* = 0 \Rightarrow (1 - 11.12k^2 - 0.01k)x_1^2 + (1 - 11.12k^2 - 0.01k)x_2^2 = 0 \qquad (18)$$

Now let's recall that $x_1 = \Delta i_d$, $x_2 = \Delta i_q$. We want the changes in the d axis (which is responsible for the real power) to be independent on the changes in the q axis (which is responsible for the reactive power). In other words, the

input u must make two independent state variables x_1 and x_2. Having taken this in mind and in order the equation (18) to be true for every t, then the optimal solution should be as:

$$1 - 11.12k^2 - 0.01k = 0 \Rightarrow k \approx \pm 0.3.$$

We keep the negative sign and hence the control law is:

$$u_1 = -x_1, u_2 = -x_2.$$

A very simple equivalent series controller for i_q is:

$$Gc(s) = -\frac{0.15}{s} \tag{19}$$

4. Nonlinear System Simulation Results

The system as shown in Figure 1 has been simulated now with the addition of an SVC placed at the bus 1. The SVC voltage controller is given by the equation (17) and the i_q controller the grid side converter in each WT of the WP is given by the equation (19). As previously, there is a step increase in the wind speed from 8 m/sec to 14 m/sec at t = 50 sec and at t = 75 sec the large induction load with the asynchronous motors is activated. Figure 13 shows the rms value of the load voltage at bus 4. The real power produced from the WP is the same as in Figure 3. The reactive power from the WP is shown in Figure 14.

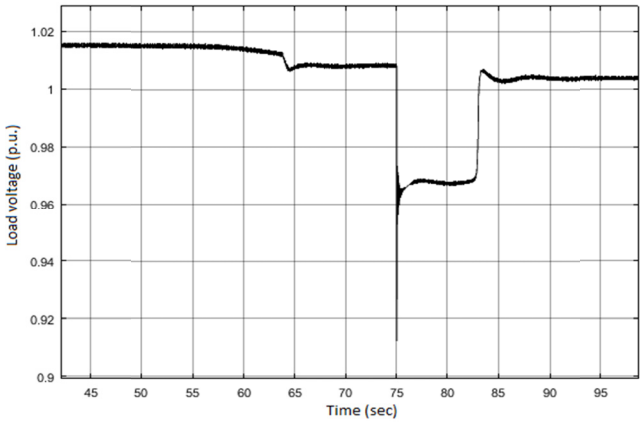

Figure 13. Load voltage with the proposed controllers

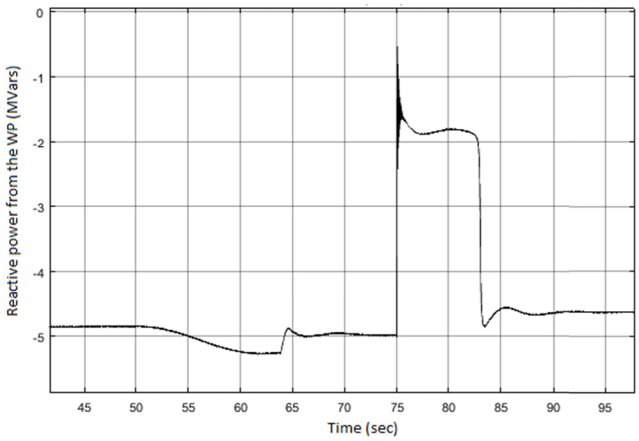

Figure 14. Reactive power towards the WP with the proposed controllers

There is an important improvement in the load voltage. The reactive power demanded by the WP causes now only almost 1 % voltage drop in the system and the reactive power towards the WP does not change direction under the start of the large motors. The voltage drop is about 4 % under the demands for reactive power both from the WP

and the inductive load during the transient period and almost zero in steady state. Besides, the time duration of the voltage drop for the starting of the motors has been decreased from 15 seconds to less than 10 seconds.

The d component of the grid-side converter current i_d is shown in Figure 15 and the q component of the grid-side converter current i_q is shown in Figure 16. We can actually see that the two components are independent one from the other and the i_d is mostly responsible for the real power output while the i_q for the reactive power of the machine.

The proposed control strategy permits the addition of two more machines to be added to the WP which now has rated power as 19.5 MW. The real power coming out from the WP in this case is shown in Figure 17 and the load voltage in Figure 18.

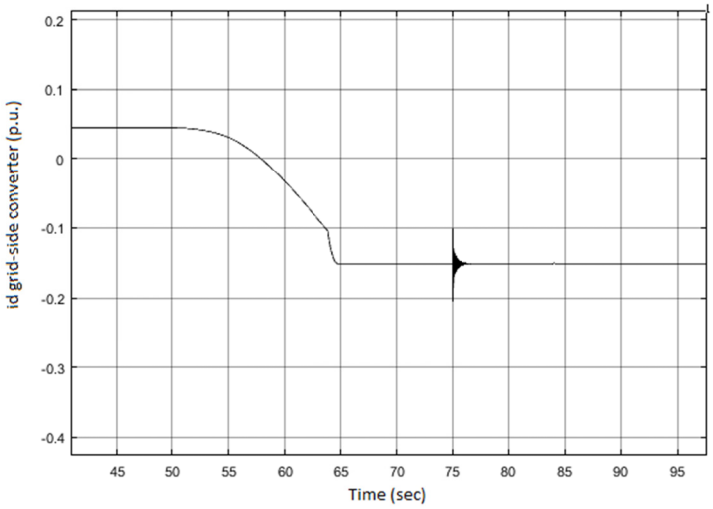

Figure 15. D component of the grid-side converter current

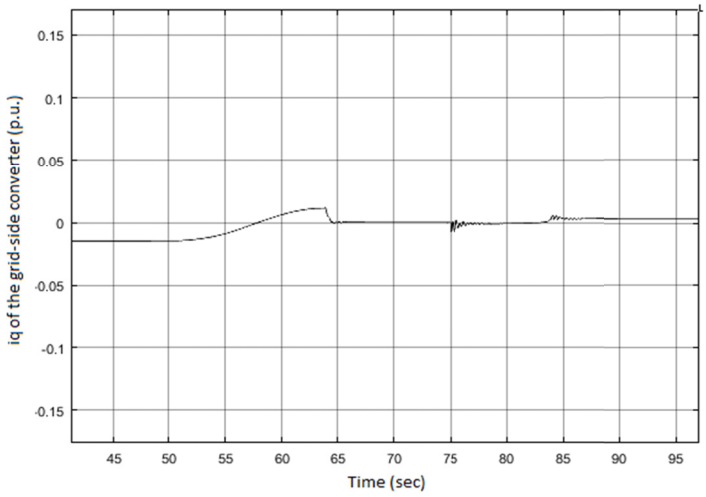

Figure 16. Q component of the grid-side converter current

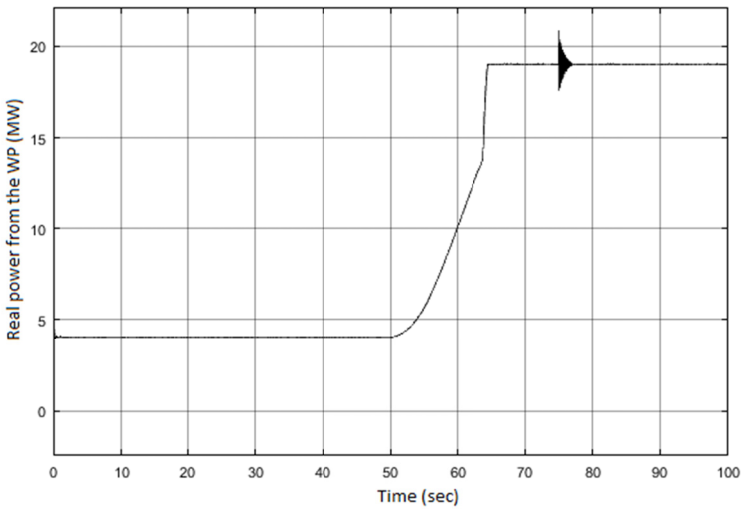

Figure 17. Real power from the WP with 13 wind turbines

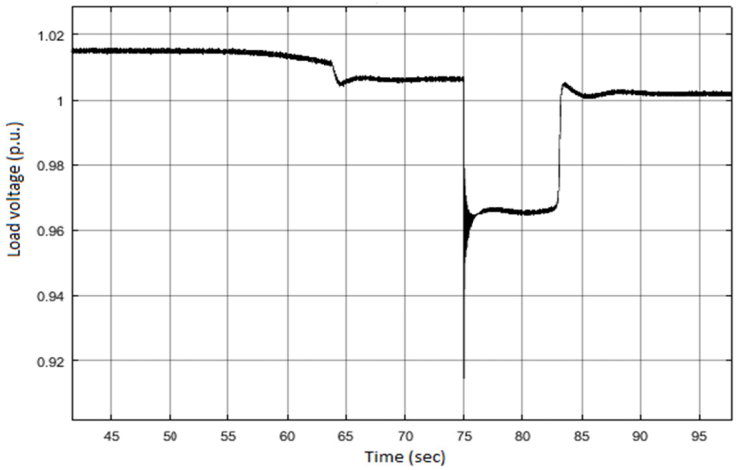

Figure 18. Load voltage with 13 wind turbines

5. Conclusions

The insertion of wind turbines with induction generators into weak systems causes extra voltage drops due to the absorbed reactive power from the generators. The low voltage may make the start of large induction motors difficult. The installation of SVC devices along with proper controllers inside the WT can improve the voltage performance in these cases. The proposed methodologies make the design of the necessary controllers easy and can be applied in any weak or local grid. The load voltage was improved significantly after the insertion of the proposed controllers into the system and the penetration of the rated real power from the wind energy was increased.

References

Custem, T. V., & Vournas, C. D. (1998). *Voltage Stability of the Electric Power System*. K. Academic.

Desineni, N. (2003). *Optimal Control Systems*. CRC Press.

Pai, M. A., & Gupta, D. P. (2016). *Small Signal Analysis of Integrated Power Systems*. Alpha Science.

Krause, P. (2010). *Analysis of Electrical Machinery.* IEEE Press.

Jahangir, H., & Hemanshu, R. P. (2014). *Robust Control for Grid Voltage Stability: High Penetration of Renewable Energy*. Springer.

Abad, G., Lopez. J., & Rodriguez, M. A. (2011). *Doubly Fed Induction Machine.* IEEE Press.

Robert, F. S. (1993). *Optimal Control and Estimation.* Dover publications.

Vijay, V., & Raja, A. (2012). *Grid Integration and Dynamic Impact of Wind Energy*. Springer.

Kesraoui, M., & Chaib, A. (2016). Grid voltage local regulation by a doubly fed induction generator-based wind turbine. *Wind Engineering, 41*(1), 13-25.

Rui, S., & Rui, X. (2015). The design and analysis of wind turbine based on differential speed regulation. *Wind Engineering, 230*(2), 221-229.

Yu, L., & Zhenlan, D. (2012). Improvement of the low-voltage ride-through capability of doubly fed Induction Generator Wind Turbines. *Wind Engineering, 36*(5), 535-551.

Appendix

Table 1. WT parameters (Abad et al., 2011)

Nominal active power P_N	1.5 MW
Nominal electrical torque T_{elN} or T_g	9555 Nm
Stator voltage V_{SN}	690 V
Nominal generator speed η_{go}	1800 rpm
Speed range of generator	900-1850 rpm
Pole pairs	4
Blades diameter d	60 m
Nominal wind speed V_{wN}	12 m/sec
Maximum power coefficient C_p	0.44
Air density	1.125 kg/m^3
Nominal turbine speed η_{to}	22.5 rpm
Speed range of turbine speed	9-23 rpm
TSR optimum	5.43
Grid side components (mΩ)	R_g = 0.33 X_g = 31.4

Table 2. Medium voltage lines

Rated voltage V_N	25 kV
Inductive reactance X_o	0.4 Ω/km
Resistance R_o	0.1 Ω/km
Length between buses 1-2	5 km
Length between buses 1-4 and 3-4	10 km

Table 3. Synchronous generator parameters (Pai et al., 2016)

Rated voltage V_N	11 kV	D axis open circuit time constant T_{do}'	4.5 sec
Rated power S_N	50 MVA	Q axis open circuit time constant T_{qo}'	0.67 sec
Transient reactance on d axis X_d'	0.25 p.u.	Inertia constant H	0.87 sec
Reactance on d axis X_d	1.65 p.u.	Stator resistance R_s	0.0045 p.u.
Transient reactance on q axis X_q'	0.46 p.u.	Power angle operating point	$\delta_o = 30^0$
Reactance on q axis X_q	1.59 p.u.	Bus 1 voltage operating point	V_{1qo}=-0.052 p.u.
Subt. int.voltage on q axis Eq' operating point	E'$_{qo}$=0.68 p.u.	Line current on D axis operating point	I_{Do}=0.28 p.u.
Subt. int.voltage on d axis Ed' operating point	E'do=0.22 p.u.	Line current on Q axis operating point	I_{Qo}=-0.1 p.u.